AIMS Materials Science, 10(2): 213–226.
DOI: 10.3934/matersci.2023012
Received: 30 October 2022
Revised: 26 December 2022
Accepted: 02 January 2023
Published: 01 February 2023

http://www.aimspress.com/journal/Materials

Research article

Ultrasonic soldering of Al_2O_3 ceramics and Ni-SiC composite by use of Bi-based active solder

Tomáš Meluš[1,*], Roman Koleňák[1], Jaromír Drápala[2], Paulína Babincová[1] and Matej Pašák[1]

[1] Faculty of Materials Science and Technology in Trnava, Slovak University of Technology in Bratislava, Jána Bottu No. 2781/25, 917 24 Trnava, Slovak Republic
[2] Faculty of Materials Science and Technology, Technical University of Ostrava, 17. Listopadu 15,708 33 Ostrava, Czech Republic

*** Correspondence:** Email: tomas.melus@stuba.sk.

Abstract: The aim of this research was to study the interaction and solderability of Al_2O_3 ceramics and Ni-SiC composite by use of an active solder type Bi11Ag1.5Ti1Mg. The chemical composition of the solder is 86.5 wt% Bi, 11 wt% Ag, 1.5 wt% Ti, 1 wt% Mg. Soldering was performed by ultrasonic activation. This solder has a wide melting interval with the initial melting temperature of 263 ℃, what corresponds to the eutectic reaction. The liquidus temperature of this solder was determined at 437 ℃. The bond between the ceramic and the solder is formed by the interaction of the active metals Bi, Ag and Mg with the surface of the substrate Al_2O_3. The thickness of the Mg reaction layer at the interface was approximately 0.8 μm. The bond at the interface between Ni-SiC and solder was formed due to the interaction of the active metals Bi, Ag, Mg and Ti. Feasibility of Bi11Ag1.5Ti1Mg solder was assessed on the basis of analyses of joint boundaries and joint shear strength measurements. The average shear strength of Al_2O_3/Bi11Ag1.5Ti1Mg/Ni-SiC joint was 54 MPa.

Keywords: soldering; Al_2O_3 ceramic; Ni-SiC substrate; Bi solder; ultrasonic soldering

1. Introduction

Electronic industry is one of the most rapidly progressing branches and it is supposed that this trend will continue. The electronic parts are during their entire life repeatedly exposed do diverse

thermal and mechanical loading. The Al_2O_3 ceramic is applied in a wide scope of power electronics. This concerns the substrates with the best power-output ratio. It is extensively applied also in the high-frequency and micro-wave technology. It is generally used for the medium and low performance, as common elements of power electronics, for example the elements of automotive electronics, control power modules, elements of photo-voltaic electronics and also Peltier's cells [1].

In recent decades also the nanocomposites are widely applied in electronic, chemical and engineering industries. The metal matrixes of nanocomposites are incorporated to nanoceramic particles (i.e. Al_2O_3, TiN, SiC and AlN). The purpose of nanoceramic particles is to enhance the microhardness and mechanical properties of metallic parts and to improve their corrosion resistance [2–7].

The Ni-SiC composite is often used in electronic devices as the multilayer ceramic capacitors, dielectric materials with nickel electrodes or composite ultra stable cathodes for charging the lithium-ion batteries.

Many scientists and research workers in university workplaces have started to search the most suitable substitute for the high-lead PbSn alloys. This fact has led to an immense development of new high-temperature soldering alloys and improvement of the existing ones [8–16].

Other substitutes for Pb-Sn solder include Zn-based solder designed for higher application temperatures. A study by the authors [9] deals with flux-free ultrasonic brazing of a Cu substrate in air by means of zinc-based solders designed for use at higher application temperatures. The soldering temperature in this case was chosen to be 20 ℃ higher than the liquidus temperature of the mentioned solder. The melting temperature of the Zn4Al solder was 404.9 ℃ and that of the Zn6Al6Ag solder was 396.9 ℃. The microstructures of the soldered joints were investigated, where a Cu_5Zn_8 phase was observed at the solder/substrate interface in the case of Zn4Al solder. The shear strength of the solder joints was 34.5 MPa in the case of Zn4Al solder and 39 MPa in the case of Zn6Al6Ag solder.

Zn-based solder designed for use at higher application temperatures has also been considered in a study [10]. The aim of the work was the manufacturing of SiC solder joints using two solders (Zn5Al3Cu and Zn5Al) using ultrasonic soldering technology. The highest achieved shear strength of the joints for both solders was approximately 139 MPa during the ultrasonic exposure time of 20 s.

Au-based high temperature solders can also be substituted for high Pb solder. Gold is classified as one of the safest chemical elements, but its disadvantage is its higher price. In the study [11], the authors deal with the soldering of a ceramic SiC chip to a Mo substrate using Au80Sn20 solder at a soldering temperature of 320 ℃. The results show excellent reliability and performance of the soldered SiC chips, which can maintain excellent performance for 2000 h at an operating temperature of 280 ℃ and 500 heating and cooling cycles. This Au-based soldering method demonstrates its potential application in high-performance SiC chips.

Research in the field of active solders has considerably expanded within recent years, what is proved also by the new studies of various foreign authors, who have dealt with the wettability research of alloys type Bi-Ag.

The authors in studies [15–18] suppose, that these alloys (type Bi-Ag) will be technologically applicable, regarding the requirements for improvement in the most demanding conditions in electronic equipments.

The most recent studies have proved that the ultrasonic soldering supports the formation of reaction products in the interface of soldered materials. Ultrasonic soldering is mostly employed in

electronics, but also in automotive, space, aviation and power industries.

Ultrasonic soldering is the process destined for joining hard-to-solder materials [19,20]. The ultrasonic power applied to molten solder causes a rapid formation of cavitation bubbles, creating thus the localized zones with extremely high temperature and pressure, which subsequently remove the surface oxide layer and improve solder wettability [21].

The research described in this article is oriented to application of soldering alloys destined for higher application temperatures based on Bi-Ag-Ti-Mg. This solder was used for soldering Al_2O_3 ceramics and Ni-SiC composite material. The joint microstructure was studied, analyses of joint interface were performed and the shear strength of joint was measured.

2. Materials and methods

The ultrasonic equipment type Hanuz UT2-ultrasonic transducer was applied, which makes use of an oscillation piezo-electric system with a titanium sonotrode, Ø3 mm in diameter. Ultrasound parameters are given in Table 1. For heating of soldering alloy, the hot plate type CERAN 500 was applied.

Table 1. Ultrasound parameters.

Parameters	
Ultrasound power	400 W
Work frequency	40 kHz
Amplitude	2 μm
Soldering temperature	380 ℃
Time of ultrasound acting	5 s

Soldering procedure consisted of degreasing the Al_2O_3 and Ni-SiC substrates, which are laid on the hot plate. Heating of the hot plate is set in accordance with the melting point of the soldering alloy used. The joints were fabricated by use of Bi-Ag-Ti-Mg-based active solder and its chemical composition is given in Table 2. Subsequently a small amount of solder was deposited on substrate surface. Another step consisted in immersion of sonotrode of ultrasonic equipment into the molten solder for the time of 5 s. The solder is activated due to effect of ultrasonic waves and the oxides rising on the solder surface are gradually disrupted. The substrates with molten solder prepared in such a way are then brought together and the joint was thus formed. The joint was then cooled down at room temperature. Figure 1 shows the schematic procedure of ultrasonic soldering.

Table 2. Chemical composition of solder.

Solder designation	Chemical composition of solder (wt%)
Bi11Ag1.5Ti1Mg	86.5% Bi, 11% Ag, 1.5% Ti, 1% Mg

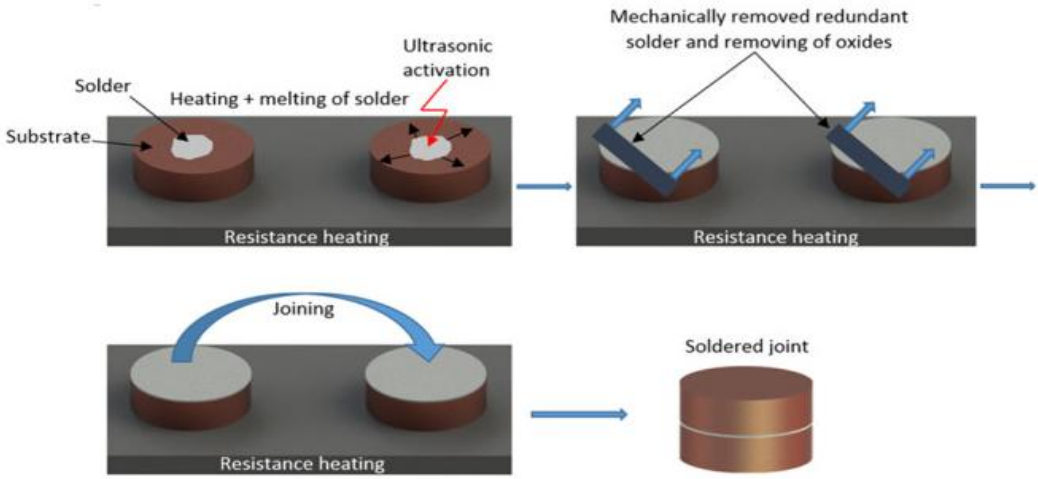

Figure 1. Shows a schematic procedure of ultrasonic soldering.

The metallographic preparation consisted of grinding and polishing processes and final etching of embedded specimens. The specimens were inserted to a jig of grinding equipment. Grinding of specimens was performed on the diamond emery papers with the granularity of 600, 1200 and 2400. During grinding process, the water was supplied to emery paper, ensuring the washing away of debris. Grinding process with each paper granularity lasted 3 min.

After grinding of specimens, the polishing process followed on the polishing discs with diamond emulsions with 9 μm, 6 μm, 3 μm and 1 μm size of particles, which lasted 10 min with each emulsion. Polishing was followed with etching process. The etchant type HCl:HNO_3 was used with concentration 1:3, for etching time of 1 s.

The substrates of following dimensions were used for soldering:

- Ni-SiC composite in form of a disc in diameter Φ 15 mm × 3 mm
- Al_2O_3 ceramics in form of s disc in diameter Φ 15 mm × 3 mm

A schematic of a solder joint for solder/substrate interface analysis is shown in Figure 2a, and a schematic for shear strength measurements is shown in Figure 2b.

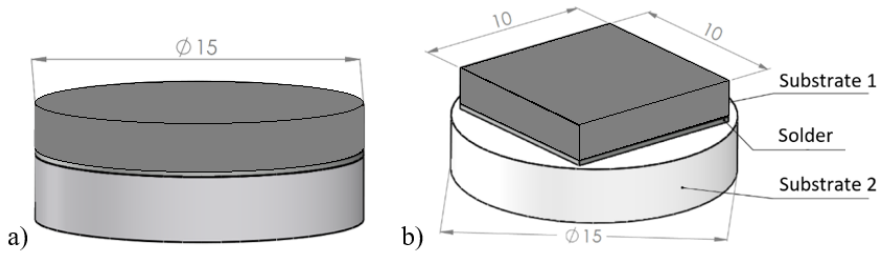

Figure 2. Solder joint assembly (a) for solder/substrate interface analysis, (b) for shear strength measurement.

The mechanical test was aimed at determining the tensile strength of the Bi11Ag1.5Ti1Mg type active solder alloy. Three test bodies were used to measure the tensile strength in the experimental solder. The specimens for tensile test had normalized shape and normalized dimensions as shown in

Figure 3. The test bodies are flat and their thickness is 4 mm. All dimensions are given in mm. The tensile strength was measured on a LabTest 5.250SP1-VM type universal tearing machine. The loading rate of the specimen was set at 1 mm/min.

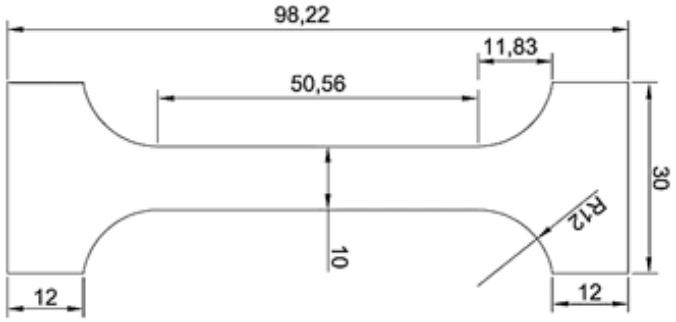

Figure 3. Shape and dimensions of the test body for tensile strength measurement.

The shear strength was determined on a LabTest 5.250SP1-VM universal tearing machine. A jig with a defined test specimen shape was used to change the direction of the loading force applied to the test specimen (Figure 4). This shear jig ensures a uniform shear load in the solder/substrate boundary plane. Three joints were used to measure the shear strength.

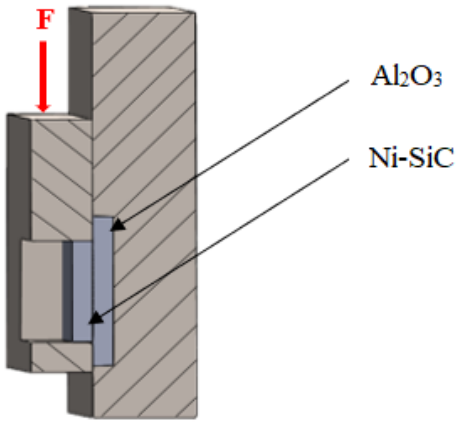

Figure 4. Schematic representation of the fixture for shear strength measurement.

The melting temperature of the solder alloy was measured by differential thermal analysis (DTA). The analysis was performed on a SETARAM Setsys 18TM DTA machine. The analysis of the structure of the interface between the solder and the substrate was carried out by scanning electron microscopy (SEM) on a TESCAN VEGA 3. The chemical element analysis was performed via the Oxford Instruments X-Max silicon drift detector, energy dispersive X-ray spectrometer (EDS, Oxford Instruments plc, Abingdon, UK).

3. Results

3.1. Microstructure analysis

The results of quantitative analysis of Bi11Ag1.5Ti1Mg solder are shown below in Figure 5. Analysis performed in Spectra 1 to 2 showed 26 wt% Mg, 27 wt% Bi, and 47 wt% Ag (big grey constituents). The dark constituents of non-convertible shape (Spectra 3 to 4) have contained the same elements but in different proportions, namely 31 wt% Mg, 19 wt% Bi and 50 wt% Ag. This phase may be described by the formula $Ag_5Mg_3Bi_2$. In Spectra 5 to 6, 11 and 12 only bismuth and titanium occurred in proportion Bi:Ti = 53:47. By phase diagram, the intermetallic phase type Ti_8Bi_9 is concerned.

Also, a ternary eutectic of lamellar type with a high proportion of Bi, with approximately 10% Ag and approximately 3.5% Mg (Spectra 7 to 8) was observed. The bright zones of matrix contain pure bismuth (Spectra 9 to 10).

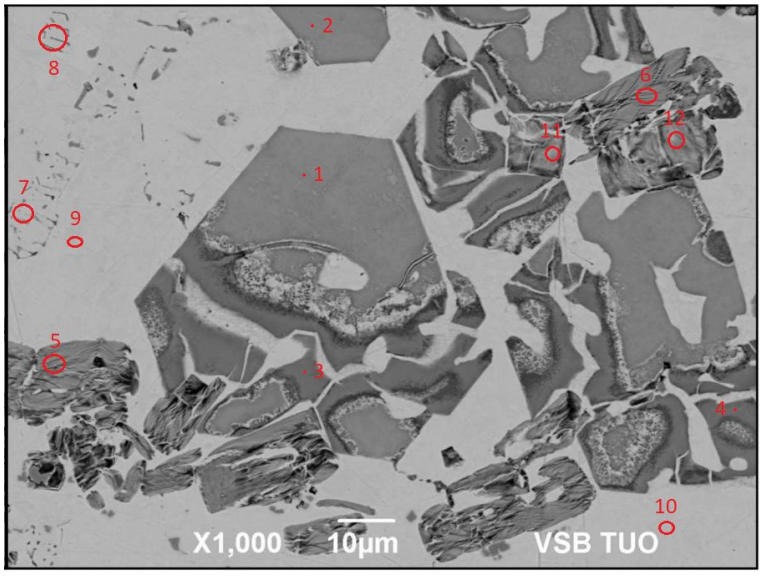

Spectrum	Mg (wt%)	Ti (wt%)	Ag (wt%)	Bi (wt%)	Solder component
Spectrum 1	25.9	0	47.4	26.7	Ag (Mg + Bi) phase
Spectrum 2	24.6	0	47.4	28.0	Ag (Mg + Bi) phase
Spectrum 3	31.0	0	50.9	18.1	$Ag_5Mg_3Bi_2$ phase
Spectrum 4	31.9	0	48.2	19.9	$Ag_5Mg_3Bi_2$ phase
Spectrum 5	0	49.0	0	51.0	Ti_8Bi_9 phase
Spectrum 6	0	43.7	0	56.3	Ti_8Bi_9 phase
Spectrum 7	3.5	0	9.1	87.5	Eutectic Bi + (Ag, Mg)
Spectrum 8	3.8	0	11.3	84.9	Eutectic Bi + (Ag, Mg)
Spectrum 9	0	0	0	100.0	Bi
Spectrum 10	0	0	0	100.0	Bi
Spectrum 11	0	45.2	0	54.8	Ti_8Bi_9 phase
Spectrum 12	0	47.5	0	52.5	Ti_8Bi_9 phase

Figure 5. Microstructure of Bi11Ag1.5Ti1Mg solder.

3.2. DTA analysis

The main aim of DTA analysis was to determine the melting interval. It resulted in DTA curve, what is actually the graph of thermal flow. The Bi11Ag1.5Ti1Mg solder (Figure 6) has the melting interval of 263 °C, what corresponds to eutectic reaction. At the first heating, the zones related with gradual dissolving of Ag-Mg-Bi and Ti_8Bi_9 phases have occurred on DTA curve, and were unanimously identified also in the structure.

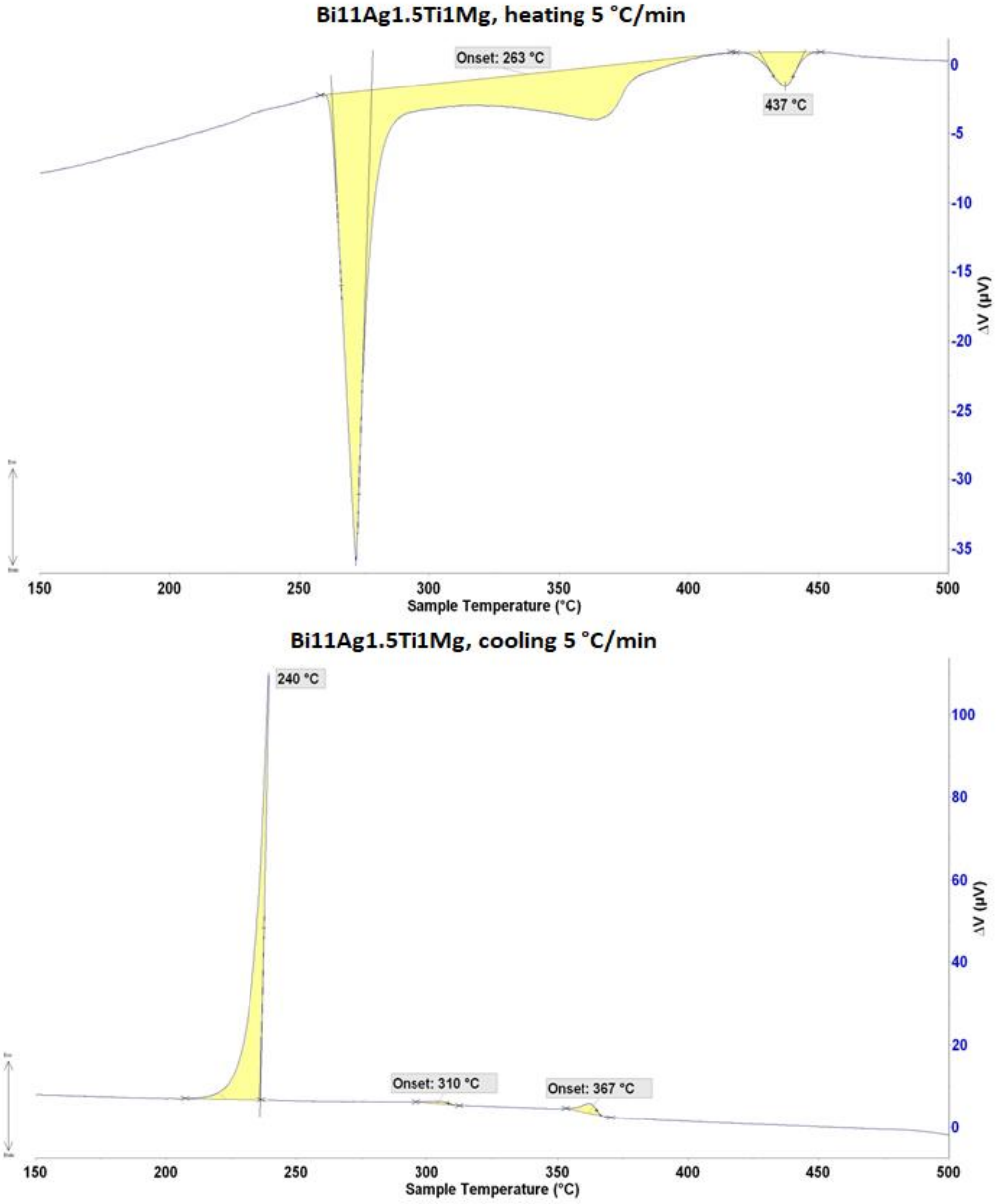

Figure 6. DTA analysis of Bi11Ag1.5Ti1Mg solder.

At the second heating, such a significant thermal effect was not manifested, due to structural changes after a slow cooling down. The significant temperatures of phase transformations in soldering alloy type Bi11Ag1.5Ti1Mg, determined by DTA analysis, are documented in Table 3.

Table 3. Significant temperatures of Bi11Ag1.5Ti1Mg solder.

Bi11Ag1.5Ti1Mg	Onset point 1	Onset point 2	TL
heating	263	-	437
cooling	240	310	367

3.3. Strength measurement of solders

Mechanical test was aimed at determination of tensile strenght of the active soldering alloy type Bi11Ag1.5Ti1Mg. Three specimens of experimental solder were used for tensile strength measurement. The loading rate was set to 1 mm/min.

The results of values measured with the given alloy are shown in the graph (Figure 7). For comparison of Bi11Ag1.5Ti1Mg solder, the measurement was performed also on a ternary solder type Bi11Ag1Mg, in order to compare the effect of added element on the resultant strength of experimental alloy. The ductility of the test bodies ranged from 0.56 to 0.63%.

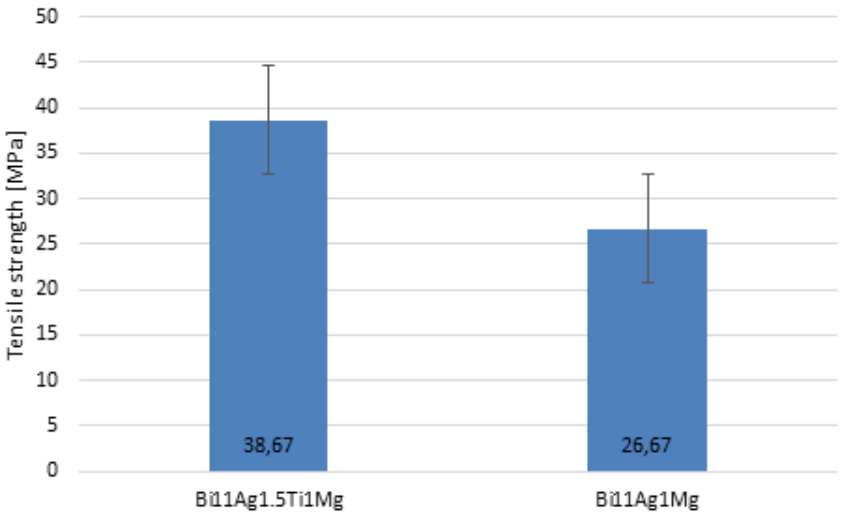

Figure 7. Tensile strength of experimental soldering alloys.

3.4. Interface analysis of solder joints

The analysis of interface in Al_2O_3/Bi11Ag1.5Ti1Mg/Ni-SiC joint is shown Figure 8. The map of a qualitative line-up of chemical analysis clearly shows the distribution of individual elements in the interface zone of Bi11Ag1.5Ti1Mg/Ni-SiC joint (Figure 9). The Bi11Ag1.5Ti1Mg/Ni-SiC interface region is mainly composed of Bi. Whereby Ag and Ti are distributed in the form of phases that bind to the Ni-SiC composite. Magnesium forms phases with silver. The Al_2O_3/Bi11Ag1.5Ti1Mg interface region is mainly uniformly formed by Bi (Figure 10). Whereby Ag and Mg form phases that bind to the ceramic interface. Titanium is not present at the interface.

The line EDX analysis at the Bi11Ag1.5Ti1Mg/Ni-SiC solder joint interface, shown in Figure 11, accurately depicts the distribution of elements in the investigated solder joint section. At the interface of the joint, mainly Ti and Mg, which were present at the interface in the form of phases, were

excluded. The thickness of this phase at the interface in this joint was approximately 3 μm. The interface of the Al_2O_3/Bi11Ag1.5Ti1Mg joint (Figure 12) was mainly Mg. The thickness of the Mg reaction layer in this junction was approximately 0.8 μm. The presence of titanium at this interface was not identified.

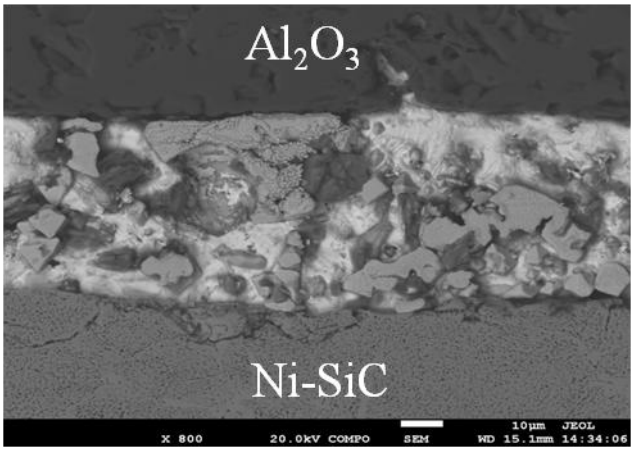

Figure 8. SEM analysis of Al_2O_3/BiAg11Ti1, 5Mg1/Ni-SiC joint.

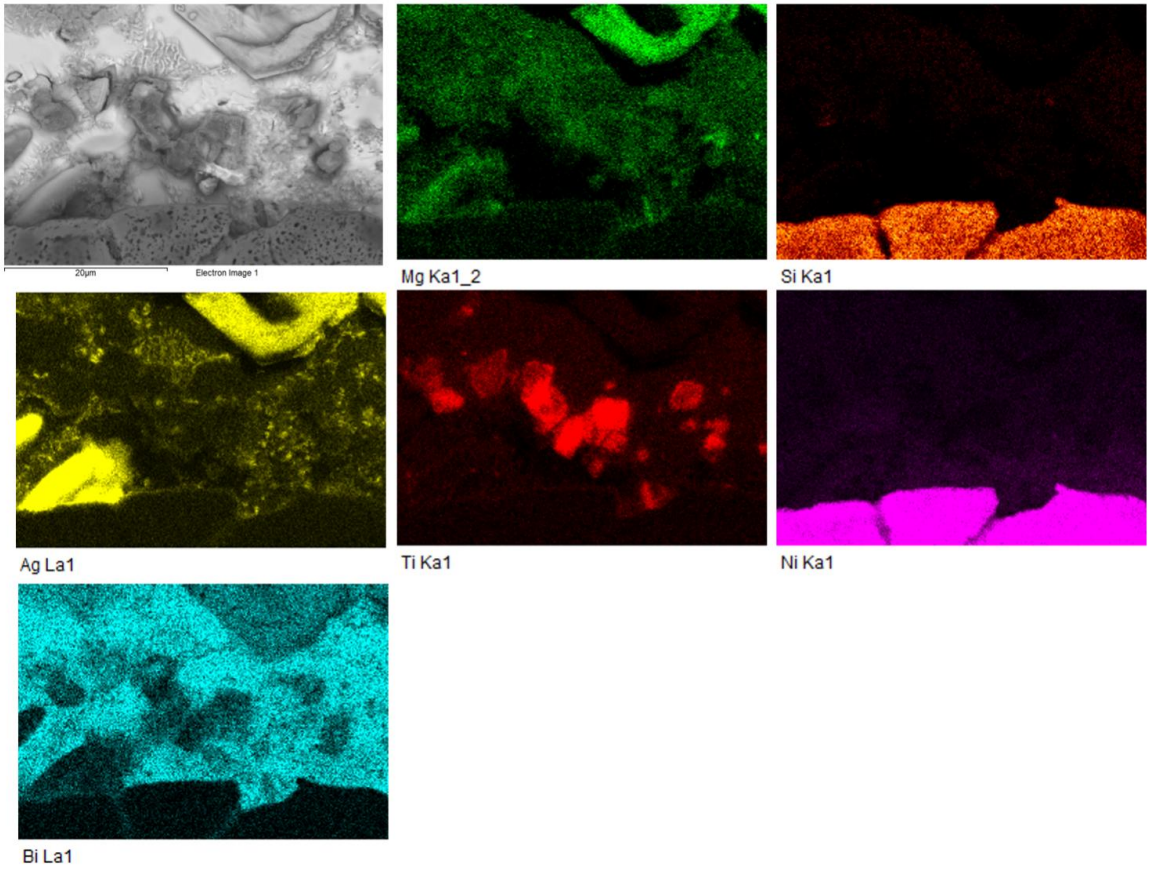

Figure 9. Planar distribution of Bi, Ag, Ti and Mg elements on the interface of Bi11Ag1.5Ti1Mg/Ni-SiC joint.

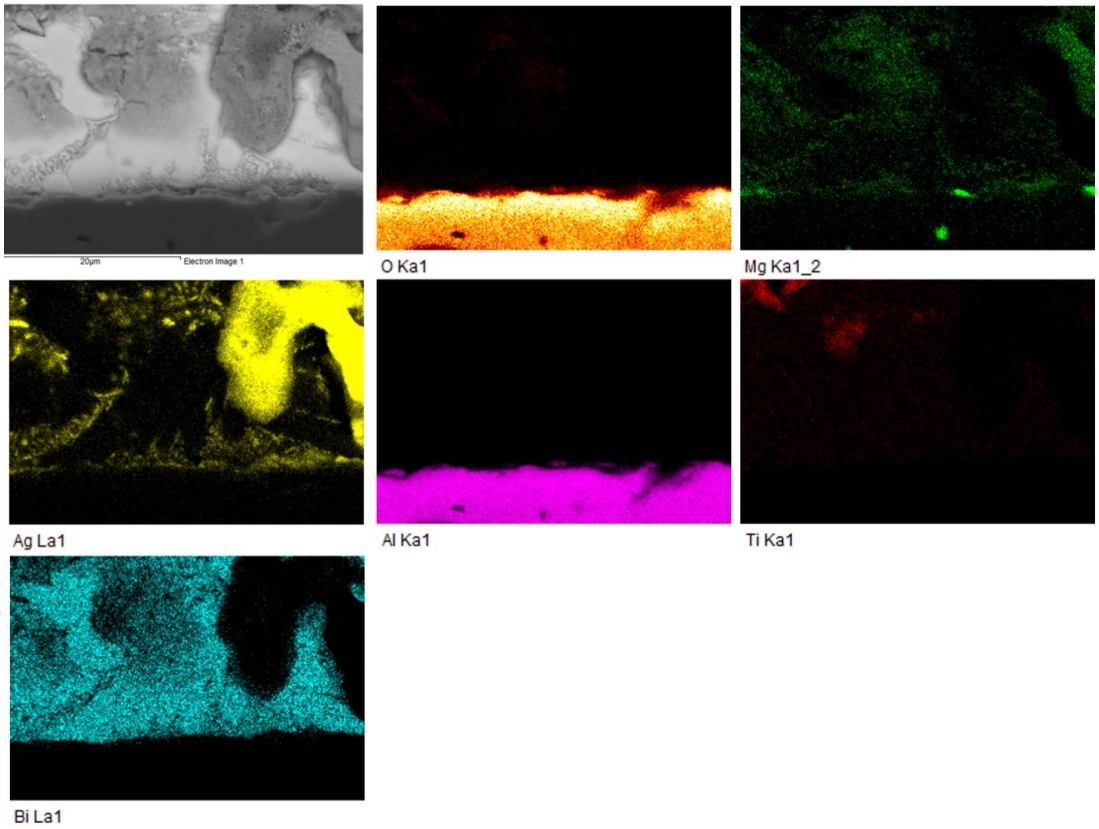

Figure 10. Planar distribution of Bi, Ag, Ti and Mg elements on the interface of Al_2O_3/Bi11Ag1.5Ti1Mg joint.

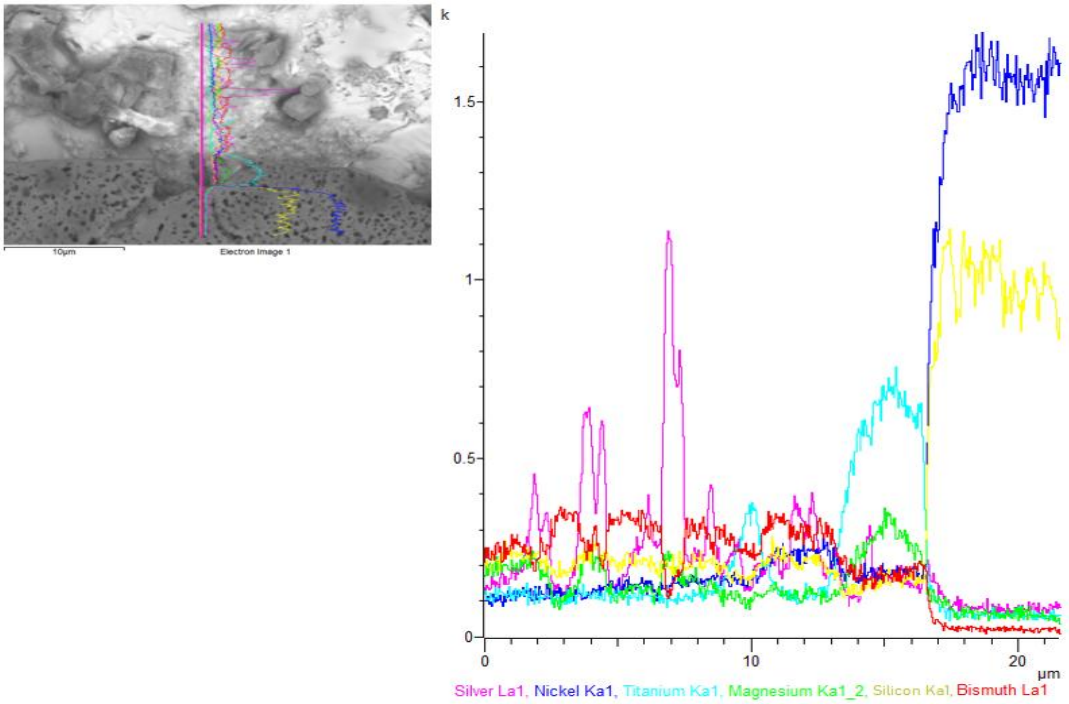

Figure 11. Line EDX analysis of BiAg11Ti1.5Mg1/Ni-SiC joint and the concentration profiles of individual elements accross the interface.

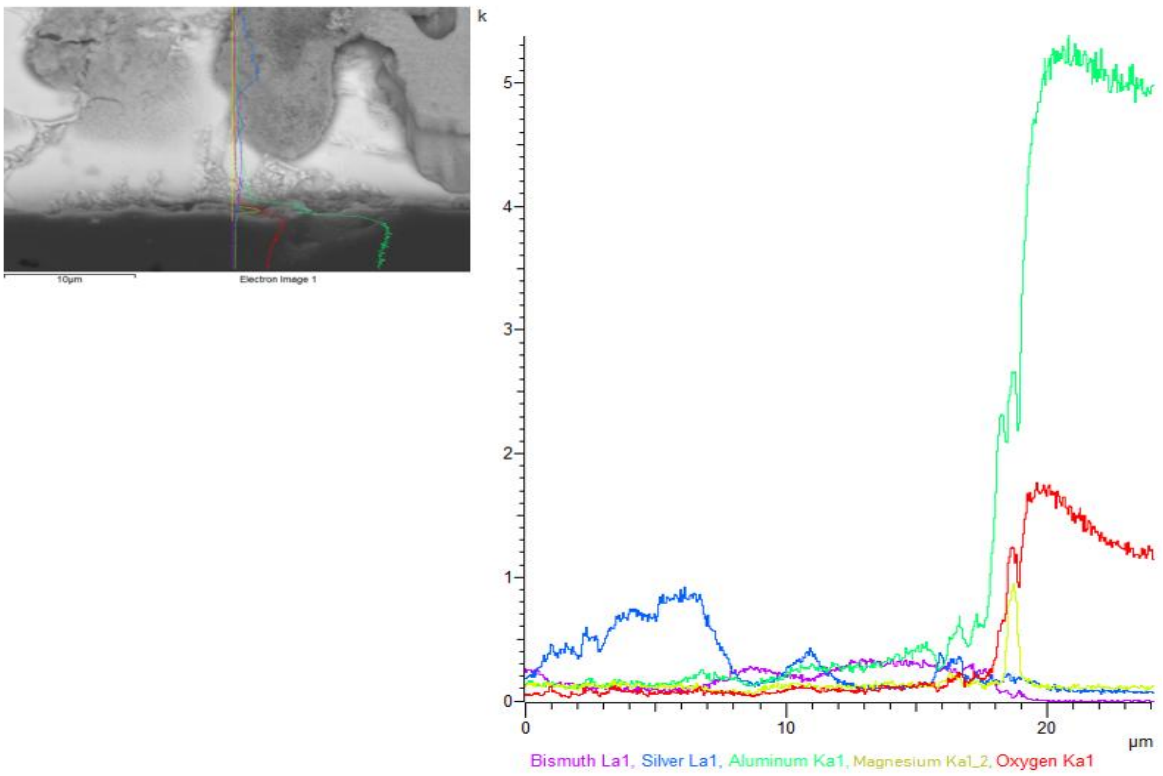

Figure 12. Line EDX analysis of Al_2O_3/Bi11Ag1.5Ti1Mg joint and the concentration profiles of individual elements accross the interface.

3.5. Shear strenght measurement

The research of this work was oriented to soldering Al_2O_3 ceramics and Ni-SiC composite. The aim of study was to assess the feasibility of an active solder type Bi-Ag-Ti-Mg.

The Al_2O_3/Bi11Ag1.5Ti1Mg/Ni-SiC solder joint has a higher strength compared to Al_2O_3/Bi11Ag1Mg/Ni-SiC solder joints due to the presence of titanium. Titanium strengthens the solder matrix. Titanium is an active element as a result of which it tends to react with other metals with which it forms various intermetallic compounds in the alloying system.

The joint of studied combination of Al_2O_3 ceramics and Ni-SiC composite fabricated by use of Bi11Ag1.5Ti1Mg solder has achieved the average shear strenght of 54 MPa (Figure 13). The results clearly show that the addition of only 1.5 wt% Ti to soldering alloy type Bi-Ag-Mg increased its average shear strength by almost half.

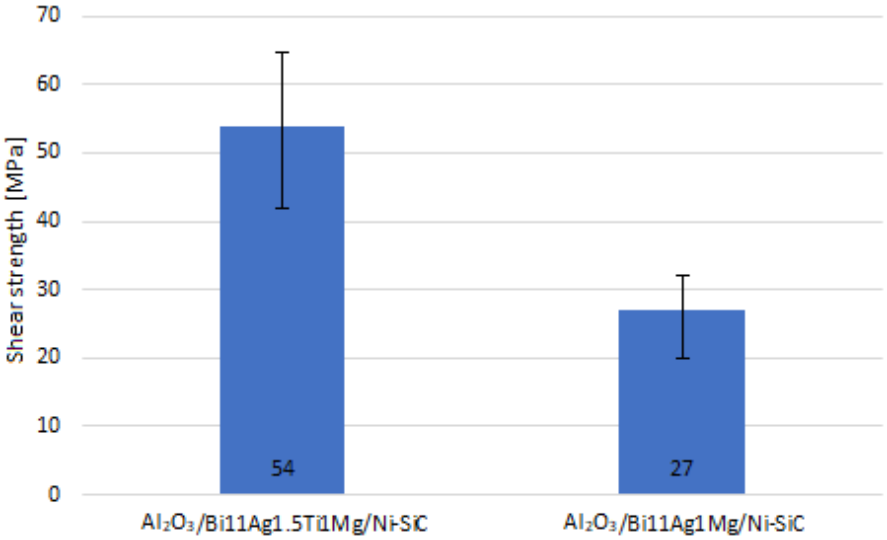

Figure 13. Shear strength measurement of solder joints.

4. Conclusions

The aim of study was to assess the feasibility of the new-developed active solder type Bi-Ag-Ti-Mg for soldering the combination of Al_2O_3 ceramics and Ni-SiC composite. This Bi-Ag-Ti-Mg-based solder belongs to the solders for higher application temperatures. Its selection is oriented to applications in power semiconductor parts.

The achieved results may be characterised as follows:

(1) The melting point of Bi11Ag1.5Ti1Mg solder and the reactions taking place during heating were determined on the basis of DTA analysis. The reaction occurs at the temperature of 263 ℃, what is related with gradual dissolution of Ag-Mg-Bi and Ti_8Bi_9.

(2) The bond at the interface of the Bi11Ag1.5Ti1Mg/Ni-SiC junction was mainly formed by Bi, Ag, Mg and Ti. The presence of active metals such as Bi, Ag, Mg and Ti ensured the wetting of the Ni-SiC substrate during the ultrasonic brazing process.

(3) The interface of the Al_2O_3/Bi11Ag1.5Ti1Mg junction was mainly formed by Bi, Ag and Mg, which are distributed at the interface in the form of phases. From the qualitative grouping map of the chemical analysis, it can be seen that titanium particles are not found at the interface of the junction with Al_2O_3 ceramic. The thickness of the Mg reaction layer at the interface was approximately 0.8 μm.

The research of joining the Al_2O_3 ceramics and Ni-SiC composite by use of Bi11Ag1.5Ti1Mg solder has proved the suitability of the selected soldering alloy. The average shear strength of Al_2O_3/Bi11Ag1.5Ti1Mg/Ni-SiC joint has attained 54 MPa.

Acknowledgments

This work was supported by the Agency for support of reseach and development on the basis of contract No. APVV-17-0025, APVV-21-0054 and VEGA project No. 1/0303/20: Research of soldering the metallic and non-metallic materials in production of semiconductor parts.

Conflict of Interest

All authors declare no conflicts of interest in this paper.

References

1. Girašek T, Pietrikova A (2015) Substrates for power electronics. *POSTERUS* 8: 16. Available from: http://www.posterus.sk/?p=18118.
2. Hashemi SH, Ashrafi A (2018) Characterisations of low phosphorus electroless Ni and composite electroless Ni-P-SiC coatings on A356 aluminium alloy. *T I Met Finish* 96: 52–56. https://doi.org/10.1080/00202967.2018.1403161
3. Ma C, Yu W, Jiang M, et al. (2018) Jet pulse electrodeposition and characterization of Ni-AlN nanocoatings in presence of ultrasound. *Ceram Int* 44: 5163–5170 https://doi.org/10.1016/j.ceramint.2017.12.121
4. Kaushal S, Gupta D, Bhowmick H (2018) On development and wear behavior of microwave-processed functionally graded Ni-SiC clads on SS-304 substrate. *J Mater Eng Perform* 27: 1–10. https://doi.org/10.1007/s11665-017-3110-z
5. Mousavi R, Bahrololoom ME, Deflorian F (2016) Preparation, corrosion, and wear resistance of Ni-Mo/Al composite coating reinforced with Al particles. *Mater Des* 110: 456–465 https://doi.org/10.1016/j.matdes.2016.08.019
6. Sun C, Liu X, Zhou C, et al. (2019) Preparation and wear properties of magnetic assisted pulse electrodeposited Ni-SiC nanocoatings. *Ceram Int* 45: 1348–1355 https://doi.org/10.1016/j.ceramint.2018.07.242
7. Zhang H, Xu F, Wang J, et al. (2022) Impact of SiC particle size upon the microstructure and characteristics of Ni-SiC nanocomposites. *J Indian Chem Soc* 99: 100474. https://doi.org/10.1016/j.jics.2022.100474
8. Krastev I, Valkova T, Zielonka A (2004) Structure and properties of electrodeposited silver-bismuth alloys. *J Appl Electrochem* 34: 79–85. https://doi.org/10.1023/B:JACH.0000005606.24413.21
9. Prach M, Koleňák R (2015) Soldering of copper with high-temperature Zn-based solders. *Procedia Eng* 100: 1370–1375. https://doi.org/10.1016/j.proeng.2015.01.505
10. Wu B, Leng X, Xiu Z, et al. (2018) Microstructural evolution of SiC joints soldered using Zn-Al filler metals with the assistance of ultrasound. *Ultrason Sonochem* 44: 280–287. https://doi.org/10.1016/j.ultsonch.2018.02.037
11. Li D, Sun D, Bi X, et al. (2022) Sintering of SiC chip via Au80Sn20 solder and its joint strength and thermomechanical reliability. *Microelectron Reliab* 128: 114443. https://doi.org/10.1016/j.microrel.2021.114443
12. Septimio R, Cruz C, Silva B et al. (2021) Microstructural and segregation effects affecting the corrosion behavior of a high-temperature Bi-Ag solder alloy in dilute chloride solution. *J Appl Electrochem* 51: 769–780. https://doi.org/10.1007/s10800-021-01533-5
13. Song JM, Chuang HY, Wu ZM (2006) Interfacial reactions between Bi-Ag high-temperature solders and metallic substrates. *J Electron Mater* 35: 1041–1049. https://doi.org/10.1007/BF02692565

14. Koleňák R, Chachula M (2013) Characteristics and properties of Bi-11Ag solder. *Solder Surf Mt Technol* 25: 68–75. https://doi.org/10.1108/09540911311309022
15. Kim JH, Jeong SW, Lee HM (2002) Thermodynamics-aided alloy design and evaluation of Pb-free solders for high-temperature applications. *Mater Trans* 43: 1873–1878. https://doi.org/10.2320/matertrans.43.1873
16. Nahavandi M, Hanim MAA, Ismarrubie ZN, et al. (2014) Effects of silver and antimony content in lead-free high-temperature solders of Bi-Ag and Bi-Sb on copper substrate. *J Electron Mater* 43: 579–585. https://doi.org/10.1007/s11664-013-2873-8
17. Šuryová D, Kostolný I, Koleňák R (2020) Fluxless ultrasonic soldering of SiC ceramics and Cu by Bi-Ag-Ti based solder. *AIMS Mater Sci* 8: 24–32. https://doi.org/10.3934/matersci.2020.1.24
18. Weber F, Rettenmsyr M (2021) Joining of SiO_2 glass and 316L stainless steel using Bi-Ag-based active solders. *J Mater Sci* 56: 3444–3454. https://doi.org/10.1007/s10853-020-05426-4
19. Lanin VL (2001) Ultrasonic soldering in electronics. *Ultrason Sonochem* 8: 379–385. https://doi.org/10.1016/S1350-4177(01)00065-7
20. Tan AT, Tan AW, Yusof F (2017) Effect of ultrasonic vibration time on the Cu/SnAgCu/Cu joint soldered by low-power-high-frequency ultrasonic-assisted reflow soldering. *Ultrason Sonochem* 34: 616–625. https://doi.org/10.1016/j.ultsonch.2016.06.039
21. Drevo EP, Nimmo KL (1994) In search of new unleaded electronic solder. *Elektron Mater* 23: 709–713. https://doi.org/10.1007/BF02651363

AIMS Press

© 2023 the Author(s), licensee AIMS Press. This is an open access article distributed under the terms of the Creative Commons Attribution License (http://creativecommons.org/licenses/by/4.0)